

Ancient and Recent Positive Selection Transformed Opioid *cis*-Regulation in Humans

Matthew V. Rockman^{1,2a*}, Matthew W. Hahn^{1,2,2b}, Nicole Soranzo³, Fritz Zimprich⁴, David B. Goldstein^{1,3,5}, Gregory A. Wray^{1,5}

1 Department of Biology, Duke University, Durham, North Carolina, United States of America, **2** Center for Population Biology, University of California, Davis, California, United States of America, **3** Department of Biology, University College, London, United Kingdom, **4** Department of Clinical Neurology, Medical University of Vienna, Vienna, Austria **5** Institute for Genome Sciences and Policy, Duke University, Durham, North Carolina, United States of America

Changes in the *cis*-regulation of neural genes likely contributed to the evolution of our species' unique attributes, but evidence of a role for natural selection has been lacking. We found that positive natural selection altered the *cis*-regulation of human *prodynorphin*, the precursor molecule for a suite of endogenous opioids and neuropeptides with critical roles in regulating perception, behavior, and memory. Independent lines of phylogenetic and population genetic evidence support a history of selective sweeps driving the evolution of the human *prodynorphin* promoter. In experimental assays of chimpanzee–human hybrid promoters, the selected sequence increases transcriptional inducibility. The evidence for a change in the response of the brain's natural opioids to inductive stimuli points to potential human-specific characteristics favored during evolution. In addition, the pattern of linked nucleotide and microsatellite variation among and within modern human populations suggests that recent selection, subsequent to the fixation of the human-specific mutations and the peopling of the globe, has favored different *prodynorphin cis*-regulatory alleles in different parts of the world.

Citation: Rockman MV, Hahn MW, Soranzo N, Zimprich F, Goldstein DB, et al. (2005) Ancient and recent positive selection transformed opioid *cis*-regulation in humans. *PLoS Biol* 3(12): e387.

Introduction

Discovering the genetic changes that accompanied the origins of modern humans and pinpointing the subset of changes driven by natural selection remain central problems in evolutionary anthropology. These changes are likely to have included changes in the complement of genes, changes in the amino acid sequences of proteins, and changes in *cis*-regulation. While divergence in gene complement [1–4] and amino acid sequence [5–9] are discernable from genome sequences, functional divergence in *cis*-regulatory regions is largely invisible in sequence data. Consequently, while we now know of many uniquely human aspects of gene complement and protein sequence, we possess only a few documented examples of human-specific *cis*-regulation [10,11]. Moreover, while statistical tests for discerning the signature of positive selection in protein-coding sequences are well developed, and genomic surveys have identified many human genes showing evidence of positive selection [12,13] or diminished negative selection [14], in only a single instance has positive selection been implicated in *cis*-regulatory divergence between humans and other apes [15]. Our ignorance of *cis*-regulatory divergence is all the more remarkable considering the importance assigned to such changes in models of evolutionary novelty [16–20]. Thirty years have passed since King and Wilson [21] argued that human evolution owes more to changes in gene regulation than to changes in gene structure, and although their theoretical justifications remain strong, empirical study of human regulatory evolution has not kept pace [22].

An understanding of the genetic basis for human traits necessarily focuses on the evolution of the brain. Inquiries into human brain-specific gene regulation have relied on phenotypic analyses, particularly microarray measurements

of gene expression in post-mortem human and ape brain tissue. These analyses document extensive differences in gene expression between humans and other great apes [23–26], but the genetic basis of such differences—if any—remains unknown. Moreover, a specific class of change in gene regulation, change in transcriptional inducibility, is invisible to studies of post-mortem tissues. Our species is distinguished by the ability to respond to and manipulate environmental cues; the responsiveness of genes to such cues, and not merely their constitutive activity, may play a role in human evolution.

Given the difficulties associated with identifying DNA sequence changes responsible for changes in inducibility, we focused on a candidate region whose role in inducibility in humans has already been demonstrated. The a priori designation of a functional regulatory element allows us to

Received July 19, 2005; Accepted September 13, 2005; Published November 15, 2005

DOI: 10.1371/journal.pbio.0030387

Copyright: © 2005 Rockman et al. This is an open-access article distributed under the terms of the Creative Commons Attribution License, which permits unrestricted use, distribution, and reproduction in any medium, provided the original author and source are credited.

Abbreviations: bp, base-pair; DRE, downstream regulatory element; DREAM, DRE-antagonist modulator; kb, kilobase; PDYN, prodynorphin; SNP, single nucleotide polymorphism

Academic Editor: Emmanouil T. Dermitzakis, The Wellcome Trust Sanger Institute, United Kingdom

*To whom correspondence should be addressed. E-mail: mrockman@princeton.edu

^a Current address: Lewis-Sigler Institute for Integrative Genomics, Princeton University, Princeton, New Jersey, United States of America

^b Current address: Department of Biology and School of Informatics, Indiana University, Bloomington, Indiana, United States of America

apply the tools of molecular evolution developed for protein sequences—specifically, rate comparisons among classes of nucleotide sites [20]. Of necessity, we also investigated the functional consequences of the species differences experimentally; we used transient transfection of promoter-reporter constructs into cultured human cells, a method with a record of success in identifying functional variation within our species [27–30].

We studied the *cis*-regulatory evolution of the opioid neuropeptide precursor prodynorphin (*PDYN*) (OMIM 131340). The opioid neuropeptides (endorphins) are the endogenous ligands for the opiate receptors. They mediate the anticipation and experience of pain [31,32], they influence behaviors including social attachment and bonding [32,33], and they affect learning and memory [32,34]. One of *PDYN*'s products is dynorphin, a peptide whose pharmacological analogs specifically affect perception [35]. A 68 base-pair (bp) tandem repeat polymorphism in the human *PDYN* promoter, 1,250 bp upstream from the start of transcription, influences the inducibility of the gene [36], and association studies have tentatively implicated the polymorphism in schizophrenia [37], cocaine addiction [38], and epilepsy [39]. These genetic associations are supported by physiological associations between *PDYN* expression and each of the phenotypes [40–42].

Results

Phylogenetic Evidence: Accelerated Evolution of a Functional Element in the Human *PDYN* Promoter

To understand the evolutionary basis for the functional variation, we sequenced 3 kilobases (kb) of *PDYN* regulatory DNA from 74 human chromosomes and 32 chromosomes from seven species of non-human primates, experimentally determining haplotypic phase by cloning each allele. The non-human primates bear a single copy of the 68-bp regulatory element, and the pattern of substitutions implies that the duplication of the element is specific to the human lineage. All human copies of the element carry five substitutions that differentiate them from the sequence inferred for the last common ancestor of humans and chimpanzees. A sixth difference is variable among repeats in some human haplotypes (Figure 1).

The five substitutions fixed on the human lineage are dramatically more than expected for 68 bp of neutrally evolving sequence. Under a model of spatially random mutation, the expected number of substitutions is fewer than 0.5, and the observed number is extremely improbable (Poisson $p < 0.0001$), whether we calculate the expectation from the density of substitutions across the *PDYN* promoter, the average divergence between human and chimpanzee on a chromosomal scale [43], or the estimated great ape substitution rate [44].

The elevated number of substitutions may be due to locally elevated mutation rate or to positive selection increasing the probability of fixation of new mutations. If the local mutation rate is intrinsically elevated, other species should also exhibit rapid evolution in the 68-bp region. We therefore tested a molecular clock, using phylogenetic likelihood ratio tests [45], to ask whether the 68-bp region is evolving rapidly due to an elevated mutation rate. The evolution of the 68-bp element is significantly accelerated exclusively along the branch leading to humans from our last common ancestor with chimpanzees ($p = 0.005$). The other branches of the evolutionary tree show no departure from rate constancy ($p = 0.657$), and the remainder of the promoter region and the coding sequence of *PDYN* also show no acceleration (Table 1). To control for possible lineage specific rate variation, we applied the relative ratio test [46], which allows for lineage-specific rates and for DNA region-specific rates, and tests for lineage-by-region interactions. Here again, the human 68-bp repeat exhibits a significant departure from the neutral expectation ($p = 0.001$ for proportionality to the rest of the promoter, $p = 0.015$ for proportionality to the coding sequence; Table 2); the remaining lineages and regions exhibit no such departures. The phylogenetic data imply that the rapid evolution of the human 68-bp element is due to positive selection.

The molecular evolution of the *PDYN* protein sequence, unlike the regulatory DNA, is consistent with a history dominated by negative selection. In a sample of the complete coding sequences from multiple chromosomes of eight primate species, 25 of the 254 amino acids in the *PDYN* protein vary, but none of the variants affect the 56 amino acids that comprise the neuroactive peptides. The exclusion of variation from the mature opioid peptides (Poisson $p = 0.004$) implies negative selection to maintain function.

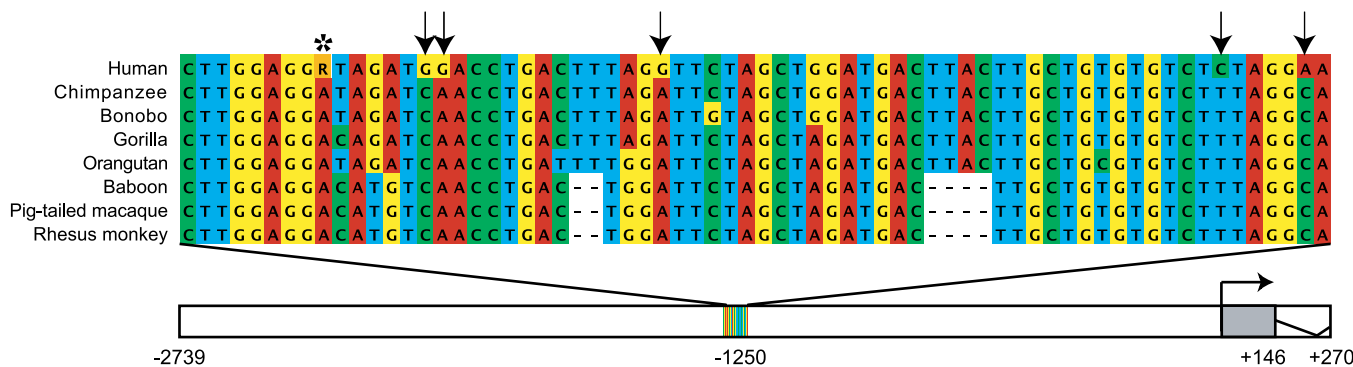


Figure 1. Divergence of the 68-bp Element in Humans

Arrows indicate five differences fixed on the human lineage. The asterisk indicates a site that varies among human repeats. In the sample of 74 human haplotypes, all one-repeat and most two-repeat alleles bear G at this site. Complete haplotype data are given in Table S1. Below, schematic of the study region showing the position of the element and the non-coding first exon with respect to the start of transcription.

DOI: 10.1371/journal.pbio.0030387.g001

Table 1. Molecular Clock Tests

Partition	Model	-lnL	Test	2 δ	df	<i>p</i>
Repeat (68 bp)	0. Molecular clock	169.40	0 versus 2	11.34	6	0.078
	1. Human branch free	165.37	0 versus 1	8.06	1	0.005
	2. All branches free	163.73	1 versus 2	3.28	5	0.657
Remainder of promoter (3,008 bp)	0. Molecular clock	5,739.90	0 versus 2	6.82	6	0.338
	1. Human branch free	5,739.89	0 versus 1	0.02	1	0.888
	2. All branches free	5,736.49	1 versus 2	6.80	5	0.236
Coding sequence (765 bp)	0. Molecular clock	1,348.52	0 versus 2	9.08	6	0.169
	1. Human branch free	1,348.51	0 versus 1	0.02	1	0.888
	2. All branches free	1,343.98	1 versus 2	9.06	5	0.107

Phylogenetic log likelihoods are compared with and without molecular clock constraints, by means of a likelihood ratio test. Only the 68-bp element shows a departure from rate constancy, and the departure is due entirely to a human-specific acceleration, as shown by the test comparing model 0 (molecular clock for all branches) to model 1 (molecular clock for all branches except the human branch). When the human specific acceleration is accommodated, the remaining branches show no departure from rate constancy (test of model 1 versus model 2).

df, degrees of freedom

DOI: 10.1371/journal.pbio.0030387.t001

Phylogenetic likelihood ratio tests found no support for positive selection shaping the amino acid sequence of the remainder of the preprotein (model 1 versus model 2 of Yang et al. [47], $p = 0.62$). Nielsen et al. [13], in a genome scan of human-chimpanzee orthologs, also found no evidence for selection on the PDYN protein. No amino acid polymorphisms are known among humans, and we found none by directly sequencing the coding regions from chromosomes bearing each of the four repeat-number alleles of the promoter.

Population Genetic Evidence: An Excess of High-Frequency-Derived Mutations Flanking the Selected Element

Positive selection alters the frequency spectrum of linked neutral mutations. As the selected mutations are driven rapidly to fixation, linked alleles are dragged along to high frequency [48]. The linked alleles may be dragged to fixation, but they may also be driven to high frequency and then decoupled from the selected mutation by recombination or allelic gene conversion. As a result, an excess of high-frequency-derived mutations flanking a fixed difference provides evidence for positive selection [49]. Our sample of 74 experimentally phased haplotypes from an Austrian population exhibits such a pattern (Table S1). Fay and Wu's

H statistic is -8.13 , strongly supporting a departure from neutrality and consistent with positive selection ($p = 0.004$). The three polymorphisms nearest to the 68-bp element have derived allele frequencies greater than 0.95 in all repeat-number allelic classes, consistent with a selective sweep that fixed mutations in the 68-bp region, and that thus predated the origin of different repeat alleles by tandem duplication. As the 68-bp element is tandemly repeated in all sampled human populations (Table 3), the signature of selection in all Austrian repeat-number allelic classes also implies that the selective events predate the global human diaspora. A sample of 20 chimpanzee haplotypes, though exhibiting many more polymorphic sites than the human haplotypes, and hence more power to detect a departure from neutrality, shows no such departure ($H = 1.62$).

The human-specific accelerated evolution of the 68-bp element is best explained as the result of positive selection favoring the fixation of mutations. Although the rate is elevated by a factor of more than ten over the neutral expectation, the selection intensity required to explain this excess is quite modest. The rate of substitution (k) is equal to the rate at which new mutations arise in the population ($2N_e\mu$) times the probability that a new mutation will become fixed [50], which is $1/2N_e$ for neutral mutations and approximately $2s$ for advantageous mutations in a population

Table 2. Relative Ratio Tests

Comparison	Model	-lnL	Test	2 δ	df	<i>p</i>
Repeat (68 bp) versus remainder of promoter (3,008 bp)	0. Relative ratio	5,908.60	0 versus 2	22.20	14	0.075
	1. Human branch free	5,903.18	0 versus 1	10.84	1	0.001
	2. All branches free	5,897.50	1 versus 2	11.36	13	0.581
Repeat (68 bp) versus coding sequence (765 bp)	0. Relative ratio	1,516.18	0 versus 2	22.38	14	0.071
	1. Human branch free	1,513.20	0 versus 1	5.96	1	0.015
	2. All branches free	1,504.99	1 versus 2	16.42	13	0.227
Remainder of promoter (3,008 bp) versus coding sequence (765 bp)	0. Relative ratio	7,089.80	0 versus 2	18.66	14	0.178
	1. Human branch free	7,089.48	0 versus 1	0.64	1	0.424
	2. All branches free	7,080.47	1 versus 2	18.02	13	0.157

Phylogenetic log likelihoods are compared with and without relative ratio constraints, by means of a likelihood ratio test. Only the 68-bp element shows a departure from rate proportionality, and the departure is due entirely to human-specific acceleration. The relative ratio test asks whether the branch-specific evolutionary rates of two data partitions are proportional. The tests involving the 68-bp element reject rate proportionality for the human branch (test of model 0 versus model 1), but not for the remaining branches of the tree (tests of model 1 versus model 2). The remainder of the promoter and the coding sequence exhibit proportional rates of evolution, consistent with neutrality.

df, degrees of freedom

DOI: 10.1371/journal.pbio.0030387.t002

Table 3. PDYN Repeat Allele Frequencies

Sample	N ^a	1	2	3	4
Cameroon	82	0.02	0.61	0.35	0.01
China	76	0.03	0.88	0.09	0
Ethiopia	90	0	0.32	0.68	0
India	84	0.01	0.63	0.36	0
Italy	88	0.01	0.35	0.64	0
Papua New Guinea	90	0	0.98	0.02	0

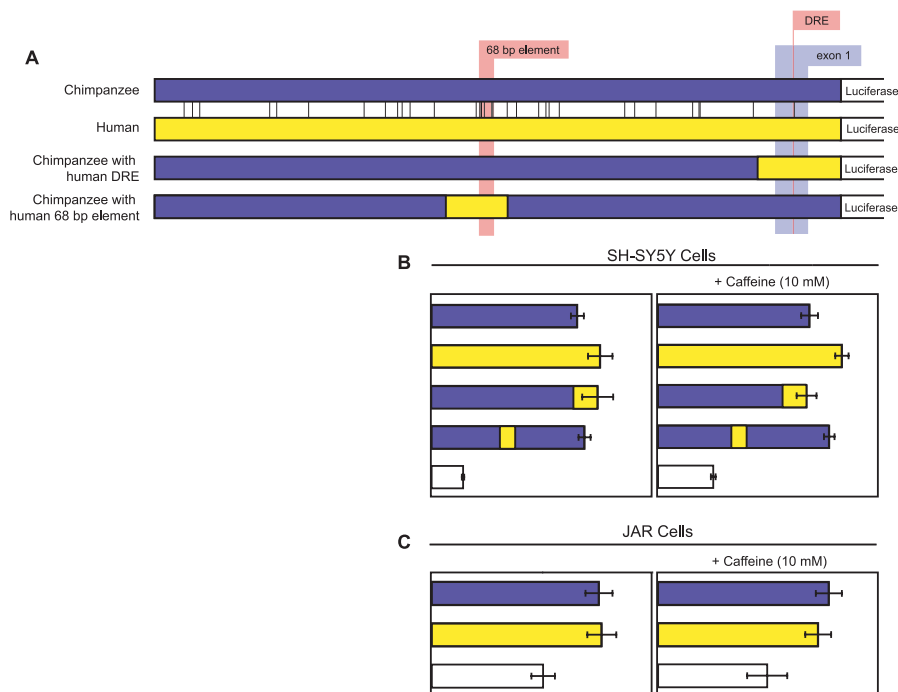
^aNumber of chromosomes sampled.
DOI: 10.1371/journal.pbio.0030387.t003

of constant size [51], where N_e is the effective population size, μ is the mutation rate, and s is the selective advantage of the mutant allele. If we let f_a be the fraction of non-deleterious mutations in the 68-bp element that are advantageous, then the rate acceleration ($k_{observed}/k_{neutral}$) is the ratio of the substitution rate in the human 68-bp element ($(1 - f_a)\mu + 4N_e s \mu f_a$) to that expected in the absence of positive selection (μ). We can place bounds on f_a by recognizing that there are only 204 base-substituting mutations possible in a 68-bp sequence. For the usual estimate [52] of long-term human effective population size, $N_e = 10,500$, s falls in the range 0.0002 to 0.045; for f_a greater than 2.2% (e.g., if all five fixed mutations were advantageous) s is less than 0.01 (Figure S1), well below the estimated selection coefficients of lactase persistence in Northern Europe [53] and G6PD deficiency [54] in regions of endemic malaria.

Functional Evidence: The Selected Element Increases Inducible PDYN Expression

To determine the effect of the selected nucleotide substitutions on PDYN transcription, we transiently transfected the human neural cell line SH-SY5Y with constructs bearing 3 kb of human or chimpanzee PDYN cis-regulatory DNA linked to a luciferase reporter. Downstream of the 68-bp repeat, in the non-coding first exon of PDYN, is a downstream regulatory element (DRE), a binding site for the repressor protein DRE-antagonist modulator (DREAM) [55]. A single nucleotide substitution in humans alters the DRE from the sequence found in the other primate species. To isolate the effect of the substitutions in the 68-bp element from the effect of the substitution in the DRE, we generated chimeric constructs containing either the human DRE or the human 68-bp element in the context of the chimpanzee promoter (Figure 2).

We found that the human DRE sequence conferred slightly elevated expression of the reporter under basal conditions, though the effect was not significant (Figure 2B; analysis of variance $p = 0.11$). The sequence of the 68-bp element has no effect under these conditions ($p = 0.66$). When the effect of DREAM is removed by stimulating the cells to release intracellular Ca^{2+} , which binds DREAM and causes it to release from DNA, the effect of the substitutions in the 68-bp element is conspicuous. Under these conditions, the human 68-bp element drives significantly higher expression than the chimpanzee sequence, regardless of the source of flanking sequence (Figure 2B; $p = 0.002$). Each relevant pairwise

**Figure 2.** The Human 68-bp Element Increases Induced PDYN Expression

We tested four 3-kb constructs, encompassing the region shown in Figure 1.

(A) The human and chimpanzee constructs differ at the sites indicated by vertical bars. The two chimeric constructs incorporated the human 68-bp element or the human DRE (DREAM binding site) into the chimpanzee construct.

(B and C) Panels show luciferase activity for each construct (\pm SEM, five to seven transfections), standardized to that observed for promoterless luciferase vectors (white bars), in SH-SY5Y and JAR cells, with and without added caffeine, which causes the release of intracellular Ca^{2+} and the release of DREAM from the DRE.

DOI: 10.1371/journal.pbio.0030387.g002

contrast is significant by *t*-test (human versus chimpanzee, 120%, $p = 0.006$; chimpanzee with human element versus chimpanzee, 115%, $p = 0.037$; human versus chimpanzee with human DRE, 120%, $p = 0.007$). In a three-factor analysis of variance, incorporating Ca^{2+} stimulation and the sequences of the DRE and the 68-bp element, the main effects of Ca^{2+} ($p < 0.001$) and the 68-bp element ($p = 0.011$) are significant and the interaction between Ca^{2+} and the 68-bp element is nearly significant ($p = 0.054$).

In contrast to the SH-SY5Y results, we observed no difference between chimpanzee and human constructs in the non-neural JAR cell line (Figure 2C), which serves as a control for the biological relevance of the *cis*-regulatory differences. Because *PDYN* is expressed in a broad range of neural and endocrine cell types and is induced by a diverse array of stimuli, our limited survey of potential functional consequences of human-specific regulatory substitutions is unlikely to have identified all such changes. Although transient transfection entails the removal of the regulatory DNA from its chromosomal context and the possible loss of biologically important interactions, the experimental results imply that the substitutions in the 68-bp element are visible to the cell.

Continuing Selection: *PDYN* Exhibits Elevated Differentiation among Populations and Reduced Variation within Them

The evidence for positive selection on the functional 68-bp element, and hence for increased *PDYN* expression in humans, raises the possibility that selection has also acted more recently on the alleles that differ in the number of tandem repeats of the element following the origin of modern humans. Intraspecific *PDYN* variation is a plausible target for selection because variation in the number of repeats has been shown to affect inducibility by the phorbol ester TPA [36] and has been associated with protection against cocaine dependency [38] and with neurological disease [37,39]. Moreover, evidence for selection among human populations would corroborate the functional importance of the 68-bp element, and hence support the inference of selection in human origins.

Population genetics predicts that recent selection in human populations will leave two types of signatures in patterns of genetic variation: departures from neutral expectations in the pattern of differentiation among populations, and departures from neutral expectations in the pattern of variation within populations. These predictions have given rise to a battery of statistical tests: F_{ST} -based tests to examine differentiation among populations, and θ -based tests to examine diversity within populations [56].

We initially genotyped the repeat polymorphism in six Old World populations and compared differentiation among populations (measured by F_{ST}) at the repeat locus to the differentiation expected at loci evolving neutrally. Elevated F_{ST} is a signature of geographically heterogeneous positive selection, driving allele frequencies to differ among populations more rapidly than they would if genetic drift and migration only were acting [57]. We estimated the neutral distribution of F_{ST} values from a set of 18 mutually unlinked candidate neutral single nucleotide polymorphisms (SNPs) typed in the same individuals [58]. Each of the candidate neutral SNPs was selected for this preliminary screening on

the basis of its high heterozygosity in Europe and its distance (more than 200 kb) from known genes. F_{ST} values are constrained by the overall level of variation at a locus, so high heterozygosity is a useful filter for a pool of informative marker SNPs. Similarly, because genes and their regulatory elements are more likely to be under selection than arbitrary non-coding DNA, SNPs distant from genes are good candidates for neutral mutations.

Alleles with one or four copies of the *PDYN* repeat element are rare in every population we examined, but the frequencies of the two- and three-repeat alleles differ dramatically among populations (Table 3). The three-repeat allele ranges in frequency from less than 10% in China and New Guinea to more than 60% in Italy and Ethiopia. The differentiation at the repeat locus is higher than all 18 neutral markers for four of fifteen pairwise comparisons (Table 4), and the degree of elevation is substantial (Figure 3A-D). Although the small number of loci in our neutral proxy dataset makes it difficult to estimate precise significance values, we may approximate a denser probability distribution by bootstrapping over loci [58]. In this test, the difference between the *PDYN* F_{ST} and the 18-locus estimate of F_{ST} is significantly higher than the bootstrapped differences ($p < 0.001$) in the four comparisons. Moreover, *PDYN* has the second or third highest F_{ST} in four more comparisons; the sum of F_{ST} ranks across all 15 comparisons is significantly low ($p = 0.01$), although this p -value cannot be taken at face value due to the non-independence of the pairwise comparisons.

If the elevated F_{ST} at *PDYN* is due to positive selection favoring different alleles in different populations, the signature of selection should also be visible in nearby variants, whose evolutionary fates are tied to the selected variant by linkage. We therefore asked whether the *PDYN* locus falls within an extended region of elevated F_{ST} . We investigated only Chinese-European F_{ST} , the population contrast for which our data suggested elevated F_{ST} (Figure 3A) and for which a genomic dataset was available. We used a dataset of 1,236,401 autosomal SNPs genotyped in African-, European-, and Chinese-Americans [59]. Because SNP ascertainment can influence the distribution of polymorphism statistics, we limited ourselves to SNPs ascertained by a single scheme: specifically, array-based resequencing of chromosomes from the National Institutes of Health Polymorphism Discovery Resource, a global sample. Because the 1.2 million SNPs share a common ascertainment bias, variation in F_{ST}

Table 4. Pairwise F_{ST} at *PDYN* and at Neutral Markers

Sample	Cameroon	China	Ethiopia	India	Italy	Papua New Guinea
Cameroon	—	0.16	0.16	0	0.12	0.30
China	0.13	—	0.50	0.15	0.45	0.19
Ethiopia	0.05	0.05	—	0.17	0	0.67
India	0.10	0.03	0.02	—	0.13	0.30
Italy	0.12	0.08	0.04	0.03	—	0.59
Papua New Guinea	0.33	0.18	0.25	0.22	0.30	—

F_{ST} at the *PDYN* 68-bp element appears above the diagonal, and F_{ST} at candidate neutral loci appears below the diagonal.

DOI: 10.1371/journal.pbio.0030387.t004

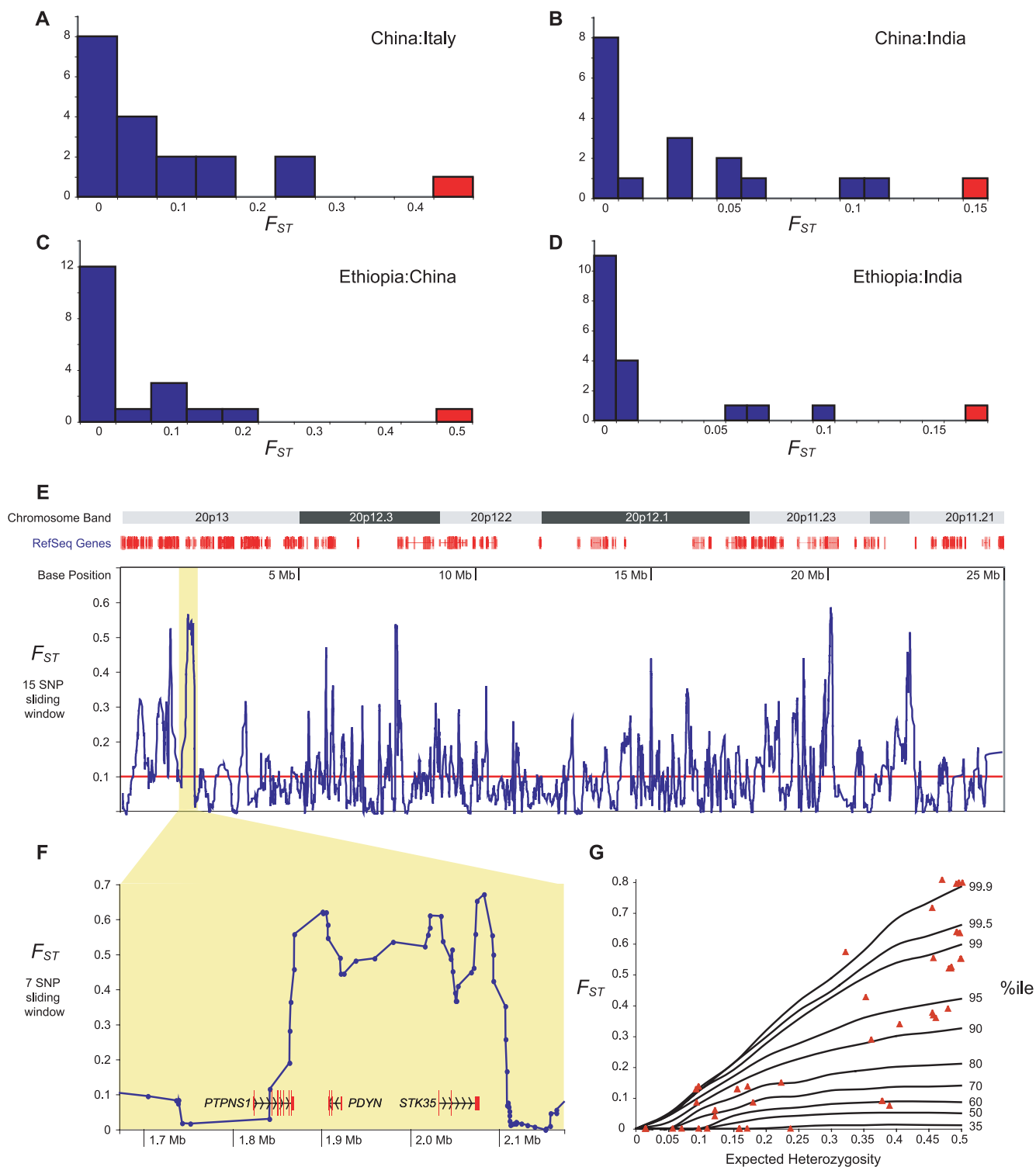


Figure 3. Elevated Differentiation at *PDYN*

(A–D) In four pairwise comparisons, F_{ST} at the *PDYN* 68-bp element (red) is markedly elevated above the F_{ST} estimated from 18 candidate neutral markers (blue) typed in the same individuals.

(E) Genetic differentiation between European- and Chinese-Americans, measured as a 15-SNP running F_{ST} average, for the entire p-arm of Chromosome 20. *PDYN* falls under a large F_{ST} peak (shaded), high above the arm average (red line). The RefSeq and chromosome band annotation is from the University of California, Santa Cruz Human Genome Browser (hg17), <http://genome.ucsc.edu> [79]. Perlegen SNP positions were matched to the hg17 assembly by the UCSC LiftOver utility.

(F) A finer-scale sliding window analysis shows that the region of elevated F_{ST} includes only two genes, *PDYN* and *STK35*, shown according to their RefSeq annotations.

(G) F_{ST} as a function of expected global heterozygosity. Red triangles represent the 52 SNPs in the Perlegen dataset in the 170-kb interval bounded by the 3' ends of *PDYN* and *STK35*. The contours define the genome-wide density of F_{ST} conditioned on heterozygosity; for each heterozygosity, the lines represent the F_{ST} of SNPs in the specified F_{ST} percentile.

DOI: 10.1371/journal.pbio.0030387.g003

along the chromosomes will reflect only variation in the demographic and selective history of genomic regions.

As an initial screen, we generated a 15-SNP sliding window plot of F_{ST} , considering only SNPs whose expected global heterozygosity exceeds 0.30. This filter is necessary to remove the dependence of F_{ST} on heterozygosity; otherwise, the plot would primarily reflect variation in the allele frequencies of the genotyped SNPs rather than differentiation among populations. As Figure 3E shows, *PDYN* falls within a tall and broad peak in F_{ST} . A finer scale sliding window plot (Figure 3F) indicates that the region of elevated F_{ST} encompasses two genes, *PDYN* and a serine/threonine kinase (*STK35*) implicated in cytoskeletal regulation [60]. These genes are divergently transcribed, and their intergenic region therefore likely contains the majority of *cis*-regulatory DNA for both genes. The 3' flanking regions of each gene also exhibit elevated F_{ST} .

The genome-wide empirical distribution of F_{ST} is shaped by both demography and selection, and therefore the tail probabilities of SNPs estimated from the empirical distribution represent a very conservative test for selection. Nevertheless, the SNPs within the *PDYN-STK35* F_{ST} peak exhibit significantly elevated F_{ST} s. In Figure 3G, we plot F_{ST} versus expected global heterozygosity for all 52 genotyped SNPs in the 170-kb interval defined by *PDYN* and *STK35* (i.e., excluding the 3' flanking SNPs). We also plot the contours of the genome-wide F_{ST} distribution conditioned on heterozygosity; note that the median F_{ST} is below 0.06 for all heterozygosities. Six of the 52 SNPs in this region (12%) have F_{ST} s in the top 0.5% of the genome-wide distribution, and 20 of the 52 (38%) are in the top 5%.

The number and location of selected variants driving elevation of F_{ST} remain unclear. However, neither *PDYN* nor *STK35* is known to contain any non-synonymous variants, and neither protein sequence exhibits evidence of positive selection during human evolution [13]. The target or targets of selection are therefore likely to be *cis*-regulatory and to include the alleles of the 68-bp element.

Positive selection driving differentiation between populations should also decrease variation within populations; as a selected allele increases in frequency, its haplotype replaces other haplotypes before accumulating new variation. Microsatellites are particularly sensitive monitors of linked selection because of their high levels of polymorphism and high mutation rate. We asked whether the microsatellite nearest the *PDYN* promoter 68-bp element, a (CA)_{13–27} dinucleotide microsatellite 1.3 kb further upstream, exhibits the predicted signatures of selection. We genotyped the microsatellite in our panel of six populations (Figure 4A), and we used repeat-number variance and expected heterozygosity as summary statistics (Table 5).

Repeat-number variance and heterozygosity are functions of $\theta = 4N_e\mu$ [61]. Because microsatellites vary in their mutation rates (μ) and recombinational contexts (which influences N_e), we used test statistics that control for these effects. For a given microsatellite, mutation rate and recombinational context are expected to be shared among populations, so they cancel out in a ratio. The ratio, $R\theta$, therefore estimates the relative effective sizes of two populations controlling for locus-specific phenomena; remaining variation among neutral microsatellites is attributable to stochastic variation in the outcomes of a neutral

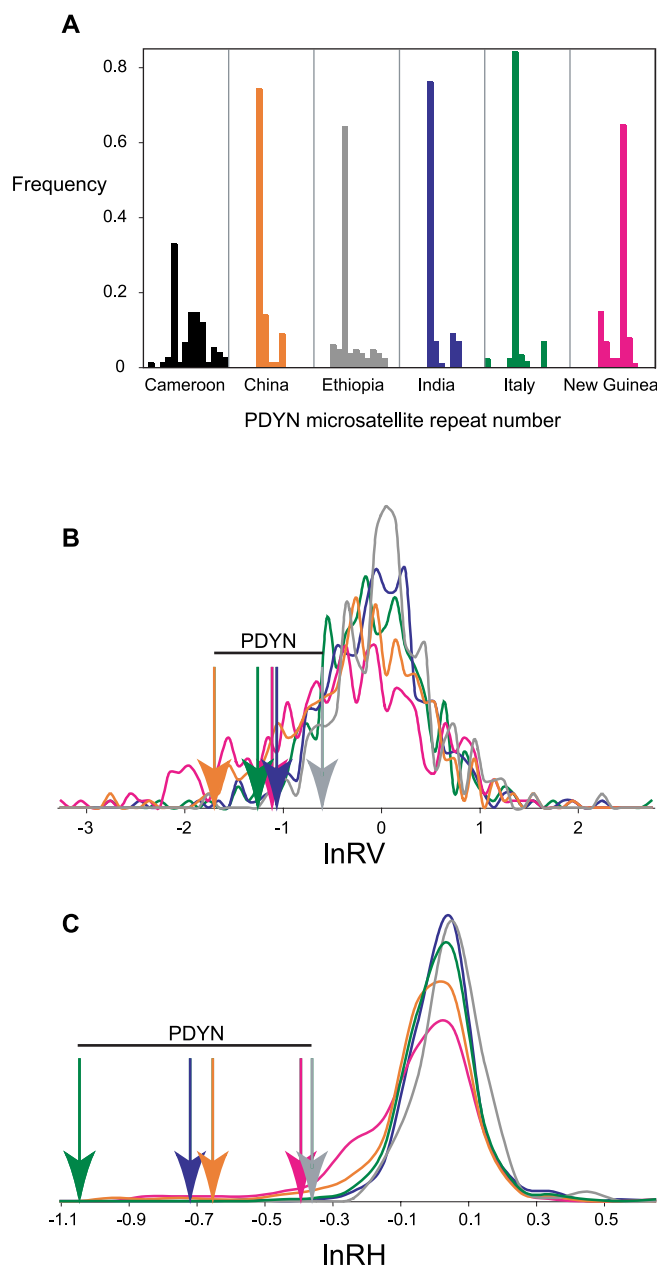


Figure 4. Altered Variation at the *PDYN* Microsatellite

(A) The allele frequency distribution of the *PDYN* microsatellite for six populations. The most common allele has 18 CA repeats in each population except Papua New Guinea, where the 22-repeat allele is most common; the overall range is 13 to 27 repeats. The distributions show a reduction in allelic variation outside of the Cameroon population.

(B) The empirical probability density of $\ln RV$ for a panel of genomically distributed microsatellites is plotted for each population, using panel A as the color key. The distributions are based on 193 microsatellite loci for Ethiopia and 377 loci for the other populations. For clarity, a single negative outlier from the New Guinea population has been omitted from the figure. The arrows indicate $\ln RV$ of the *PDYN* microsatellite for each population, in the left tails of the distributions, indicating a locus-specific reduction in repeat-number variance.

(C) The empirical probability density for $\ln RH$. Again, the *PDYN* microsatellite exhibits significantly negative $\ln RH$ values, indicating a locus-specific reduction in heterozygosity at *PDYN* in the non-West African populations.

DOI: 10.1371/journal.pbio.0030387.g004

Table 5. PDYN Microsatellite Summary Statistics

Sample	Sample Size	E(H)	Var
Cameroon	76	0.836	7.97
China	78	0.424	1.44
Ethiopia	84	0.578	4.29
India	88	0.407	2.67
Italy	88	0.289	2.33
Papua New Guinea	88	0.553	2.67
Austria 1-repeat haplotypes	10	0.533	6.67
Austria 2-repeat haplotypes	24	0.605	4.72
Austria 3-repeat haplotypes	32	0.121	0.06
Austria 4-repeat haplotypes	8	0	0
Chimpanzee	20	0.853	6.24

DOI: 10.1371/journal.pbio.0030387.t005

coalescent process [62,63]. Positive selection in one population will reduce heterozygosity and repeat-number variance at a linked microsatellite, causing it to appear in the tails of the estimated distributions of $\ln RV$ and $\ln RH$ (where repeat-number variance and heterozygosity are used in place of θ).

We estimated $\ln R\theta$ distributions empirically from a genome-wide dataset of 337 autosomal loci [64, 65]. Because our F_{ST} data do not indicate recent selection in the sample from Cameroon, we used Cameroon as the denominator in all ratios, and we tested for positive selection in the other populations. Those in which positive selection has acted are predicted to exhibit significantly negative $\ln R\theta$ at the PDYN microsatellite, unless the Cameroon sample has experienced equal or more extreme positive selection at a PDYN-linked locus.

We found a significant reduction in repeat-number variance at the PDYN microsatellite (Figure 4B) in three populations (Italy, $p = 0.031$; India, $p = 0.034$; China, $p = 0.021$), but not in Ethiopia ($p = 0.103$) or Papua New Guinea ($p = 0.209$). The sum of $\ln RV$ ranks across populations places PDYN in the 2.5% tail of lowest sums among all the microsatellites. The reduction in heterozygosity at PDYN (Figure 4C) is even more extreme ($p < 0.003$ for Italy and India, $p < 0.006$ for Ethiopia, $p = 0.016$ for China, and $p = 0.072$ for Papua New Guinea). The PDYN microsatellite is the locus with the lowest $\ln RH$ rank summed over populations.

The relationship between the events reducing variation at the PDYN microsatellite and the events elevating F_{ST} at the 68-bp repeat is most obvious when the haplotypic phase between the two elements is considered. We calculated expected heterozygosity and repeat-number variance in subsets of our experimentally determined haplotypes from an Austrian population. As shown in Table 5, the overall reduction in microsatellite heterozygosity and repeat-number variance is driven by the rapid elevation in frequency of the three-repeat allele at the 68-bp element.

The combination of elevated F_{ST} s and reduced $\ln R\theta$ s implies that the selection occurred in multiple populations, favoring the two-repeat allele in China and India, and the three-repeat allele in Italy and Ethiopia. However, it remains possible that the 68-bp element in the PDYN promoter is not itself the target of selection, as the entire PDYN-STK35 region bears the signature of recent positive selection.

Discussion

The phylogenetic and population genetic data described above are difficult to reconcile with a simple selective scenario. Instead, they point to a complex selective history at the human PDYN locus, with ancient positive selection acting across the species and more recent positive selection favoring different alleles in local contexts.

The data allow us to construct a coherent and plausible model that accounts for each observation. During the course of human descent from our last common ancestor with chimpanzees, multiple non-coding mutations arising upstream of the start of PDYN transcription altered the gene's cis-regulation and swept to fixation due to positive selection, as indicated by analysis of the primate sequence data and the elevated frequency of derived alleles flanking the fixations. Concurrently, mutations altering the neuroactive peptide products of PDYN were eliminated by negative selection. The proximate effect of the fixed cis-regulatory mutations is the upregulation of PDYN transcription, particularly when induced by intracellular calcium release. Subsequent to the selective sweeps, but prior to the peopling of the globe, the 68-bp region encompassing the fixed mutations duplicated. The timing of these events is supported by the presence of the fixed differences on all copies of the repeat, the high frequency of flanking derived mutations in all repeat-number allele classes, and the presence of the duplication in all sampled human populations. The duplication segregates today as a tandem repeat polymorphism, with one to four repeats. After the global human diaspora, human populations in different parts of the world experienced different regimes of selection on PDYN cis-regulation, as indicated by the elevated F_{ST} values. Selection drove an increase in the frequency of the three-repeat allele in Europe and East Africa and independently increased the frequency of the two-repeat allele in India and China, according to the significantly reduced $\ln R\theta$ values in each of the populations implicated by the F_{ST} data.

The convergence of independent lines of evidence—phylogenetic, population genetic, and functional evidence for ancient selection, and evidence of recent selection in patterns of variation within and among modern human populations—underscores the importance of PDYN to human biology. Though PDYN has received little attention from human geneticists, our evolutionary genetic data suggest that the locus would repay further investigation. While we may point to possible environmental and cultural agents of recent selection, including differences in use of plant opiates and environmental inducers of endogenous opioids, such as acupuncture [66], the phenotype targeted by the ancient selection is unknown.

For thousands of years, people have used opiates to alter consciousness and ameliorate pain. Our data indicate that the evolution of our species involved changes in the inducibility of an endogenous opioid precursor, and that these changes were driven by positive natural selection. Changes in neuropeptide expression are known to have accompanied behavioral evolution in other species [67,68], but the difficulties in studying such changes in gene expression in living human brains have prevented their discovery until now. PDYN, a natural candidate for human-specific traits by virtue of its documented role in perception,

emotion, nociception, and learning is the first documented instance of a neural gene whose *cis*-regulation has been shaped by positive selection during human origins. Although the transcriptional effects of the selected changes in the *PDYN* promoter appear to be subtle, slight changes in gene expression are capable of substantial effects on organismal phenotypes [69]. In keeping with the predictions of King and Wilson [21], our data imply that minor changes in gene regulation played a significant role in the evolution of the traits that make us human.

Materials and Methods

Cloning and sequencing. Our human haplotypes are from an anonymized collection of genomic DNA samples from an Austrian population [39]. To guarantee recovery of rare one- and four-repeat alleles, we selected DNAs of known repeat-number genotype (note that representative samples were chosen for population genetic analyses, described below). We PCR amplified 3-kb fragments of *PDYN* promoter from genomic DNA, using high-fidelity Phusion polymerase (Finnzymes, Espoo, Finland). For repeat-number heterozygotes, PCR products were cloned into pGL3-basic vector, using an invariant Acc65I site at the 5' end of the promoter and a NheI site incorporated into the PCR primer at the 3' end. For each haplotype, we completely sequenced multiple clones, and all singletons were verified by bidirectional direct sequencing. Repeat-number homozygotes were sequenced directly from PCR products; in cases of multiple-site heterozygosity, these PCR products were also cloned and multiple clones sequenced to determine phase. Non-human primate DNA was acquired from Coriell Repositories (Camden, New Jersey, United States) (*Pan troglodytes*, *Pan paniscus*, *Gorilla gorilla*, *Pongo pygmaeus*, *Macaca nemestrina*, and *Macaca mulatta*), and as gifts from A. Stone (*Pan troglodytes* and *Pan paniscus*), and D. Loisel (*Papio papio*). For each sample, Phusion PCR products were cloned and sequenced as above. We sequenced the two coding exons directly from PCR products. In addition to non-human primates, we included four Austrian samples with known promoter repeat genotype to ensure recovery of coding sequence linked to each repeat-number allele. Sequences were scored using Sequencher (GeneCodes Corporation, Ann Arbor, Michigan, United States).

Phylogenetic and population genetic analyses. For all tests of substitution densities and rates, we conservatively assume that the site segregating among human repeat alleles represents a new mutation within humans and not a sixth fixed difference between humans and chimpanzees. To calculate the Poisson probability of five substitutions in 68 bp on the human branch, we found the expectation by considering the local average substitution rate, the genomic average divergence from chimpanzees, or the estimated genomic average mutation rate. The local average substitution rate, estimated from the human branch length for the entire 3-kb promoter sequence, including the 68-bp element, yields an expectation of 0.46 substitutions per 68 bp. At the broader scale of whole chromosomes, human and chimpanzee differ by nucleotide substitutions at an average of 1.44% of sites [43]; if one half of the divergence occurred on the human branch, the expected number of substitutions per 68 bp is 0.49. If instead of divergence, we consider the germline mutation rate, estimated at 0.99×10^{-9} per site, and assuming 5 to 7 million years of evolution since the last common ancestor of humans and chimpanzees [44], we expect 0.34 to 0.47 substitutions per 68 bp. Note that none of the substitutions occurs in a CpG context, although CpG may have been an intermediate in the adjacent substitutions that changed CpA in non-human primates to GpG in humans. The five substitutions are C→G, A→G, A→G, T→C, and C→A, three transitions and two transversions.

Molecular clock and relative ratio tests were implemented in HYPHY (<http://www.hyphy.org>) using an eight-sequence dataset, with a single allele representing each species. As our human exemplar we used the most common one-repeat haplotype from our sample of ten Austrian one-repeat alleles; we chose a one-repeat haplotype to facilitate comparison with the one-repeat sequences of non-human primates. The most common chimpanzee haplotype represented that species, while for other species, because each haplotype is unique in our small sample, a haplotype was selected randomly. Molecular clock tests used best-fit time reversible substitution models selected using ModelTest [70]. For the coding sequence and the promoter excluding the repeat, the favored model is HKY with Γ -distributed among-site

rate variation. We used the maximum likelihood-estimated transition/transversion ratio and rate variation shape parameter and empirical base frequencies. For the repeat, the favored model is K2P. The relative ratio tests were performed using the HKY + Γ model, but results with K2P are very similar.

Negative selection on neuropeptides was tested by calculating the Poisson probability that zero of 25 variable positions would fall in the 56 of 254 amino acids comprising the neuropeptides. To test for positive selection in the remainder of the protein, we compared models 1 and 2 ($2\delta = 0.24364$, $p = 0.62$) and models 7 and 8 ($2\delta = 0.0001$, $p = 0.99$) from Yang et al. [47], in HYPHY, using the Goldman-Yang parameterization with base frequencies independent of codon position. The dataset included one sequence from each species.

For haplotype-based tests, we generated a representative population sample [71] by drawing 74 haplotypes from the sequenced Austrian haplotypes according to the population frequency of the different repeat-number alleles [36]. Summary statistics and their p -values were found using DNAsp [72].

Intensity of selection. Estimation of the rate acceleration factor (A) involves three data partitions whose evolution is consistent with neutrality. First, we found the maximum likelihood estimate of the ratio of substitution rates between the 68-bp element and the remainder of the promoter, excluding the human lineage (ratio = 1.804). Next, we estimated the substitution rate on the human lineage for the portion of the promoter excluding the 68-bp element (rate = 0.00506 substitutions per site), holding the substitution model parameters constant. The product of these gives the expectation for the human 68-bp repeat under neutrality, 0.00913 substitutions per site. (Note that the Poisson probability of five substitutions, given that expectation, is 0.00005, and three or four mutations also fall in the 0.025 tail of the Poisson probability.) The maximum likelihood estimate of the substitution rate in the 68-bp element along the human lineage, 0.0926 substitutions per site, represents an acceleration factor $A = 10.1$. All estimates employed the HKY + Γ substitution model.

The genic selection coefficient s is estimated from the relations $A = (\mu(1 - f_a - f_d) + 4N_e s \mu f_a) / (\mu(1 - f_a))$ and $f_a + f_d + f_0 = 1$, where f_a , f_d , and f_0 are the fraction of mutations that are advantageous, deleterious, and neutral, respectively. Figure S1 shows s as a function of the nuisance parameters f_a and f_d . We make the approximating assumption that f_a , f_b , and f_0 are constant over the course of the selective history of the locus.

To convert the acceleration factor to s , we consider the case of sequential fixations and ignore the effect of interference among independent advantageous mutations. The effect of interference is likely to be modest, as the expectation of the conditional fixation time of advantageous alleles, $\sim(2/s)(\ln 2N)$ [73], is less than 10,000 generations for $s > 0.002$, while the time available for fixations is roughly 300,000 generations (6 million years, 20 years per generation). Our estimate of s is based on the long-term effective population size since the divergence of humans and chimpanzees, which may be much larger than the estimate for modern humans. Larger N_e translates into even lower estimates of s . The fixation probability ($\sim 2s$ for constant N_e) is sensitive to fluctuations in effective population size [74], increasing during population expansions and decreasing during bottlenecks. Our simple approach assumes constant effective size.

The magnitude of the estimated rate acceleration excludes non-reciprocal exchange processes subsequent to duplication (e.g., gene conversion and unequal crossing-over) as possible explanations for the human-specific acceleration. Unbiased non-reciprocal exchanges do not alter substitution rates; although the number of sites available to mutate is increased by the number of repeat elements (n), the probability that a new mutation will spread among the repeats is $1/n$. Biased processes can accelerate substitution [75], but only when the bias consistently favors new mutations over ancestral alleles. Even in the most extreme case, where every inter-repeat conversion event replaces an ancestral allele with a new mutation, the maximum rate acceleration is n . In human *PDYN*, n averages less than three and never exceeds four, and the long-term effective number of repeats (the harmonic mean of repeat number over the duration of the human lineage) is likely quite close to one. Strong bias is at any rate ruled out by the presence of a segregating variant among the repeats. So non-reciprocal exchange cannot produce the observed acceleration factor under neutrality. Under positive selection, however, tandem repeats, with or without biased conversion, can increase the power of deterministic forces relative to drift by increasing the effective population size to $N_e n$ [76].

Vectors, cell culture, and transfection. We used the pGL3basic luciferase reporter (Promega, Madison, Wisconsin, United States). Chimpanzee and human constructs were generated as described above ("Cloning and sequencing"). To generate chimeric constructs with DRE site swaps, we cut the inserts with BstAPI and exchanged the DRE-containing fragments. To generate a 68-bp element chimera, we excised a human repeat using BspHI and DrdI and inserted it into a chimpanzee vector in the equivalent position. Vectors were verified by sequencing. We cultured JAR choriocarcinoma cells in RPMI 1640 with 2 mM L-glutamine and 10 mM HEPES, supplemented with 10% FBS. SH-SY5Y neuroblastoma cells were cultured in a 1:1 mixture of Ham's F-12 and EMEM with 1 mM sodium pyruvate and 0.1 mM non-essential amino acids, supplemented with 10% FBS. Both cell lines were acquired from ATCC and maintained at 37 °C with 5% CO₂. We performed transfections in 24-well plates with JAR cells at 90% confluence and SH-SY5Y cells at 50% confluence. The transfection mix, in OPTI-MEM, included 2 µl of Lipofectamine2000, 0.72 µg of pGL3, and 0.08 µg of *Renilla*-TK (Promega) as a co-reporter to control for variation in transfection efficiency. At 26 h, medium was supplemented with growth medium with or without caffeine (final concentration 10 mM). Cells were harvested 16 h later. Luciferase activity was measured using the Dual-Luciferase Reporter Assay System (Promega) and a Turner Designs 20/20 luminometer. Results are reported as ratios of firefly:Renilla luciferase, standardized by setting the pGL3-basic ratio to one. Lysates from mock transfected cells were used to blank for machine background. All transfections were performed five to seven times, and effects assessed by analysis of variance and pairwise *t*-tests.

F_{ST} and $\ln R\theta$ analysis. For the six-population analysis of F_{ST} , neutral markers, DNA samples, F_{ST} calculations, and bootstrap resampling are as previously described [58]. We genotyped the 68-bp repeat and the *PDYN* microsatellite by scoring the length of labeled PCR products run on an ABI 3700 capillary gel machine. We verified genotypes for 10% of samples by direct sequencing of PCR products.

Analysis of Perlegen data was limited to autosomal SNPs ascertained according to scheme A of Hinds et al. [59], array-based resequencing of National Institutes of Health Polymorphism Discovery Resource chromosomes. SNP data were downloaded from <http://genome.perlegen.com/browser/download.html>, and we used Perlegen's precalculated F_{ST} values. To calculate expected global heterozygosity, we averaged the allele frequencies for the three genotyped populations and used $2p-2p^2$, where p is the average frequency of the global minor allele. To generate the percentile plot for F_{ST} conditioned on expected heterozygosity, we sorted the SNPs into ten bins, each covering five percentage points of expected global heterozygosity range, we ranked SNPs within bins by F_{ST} , and then we recovered the F_{ST} for the SNP whose rank coincides with the relevant percentile within that bin. In Figure 3G, the contours are connecting the data points for the ten bins for each percentile; e.g., the point where the contours hit expected heterozygosity 0.5 represents the F_{ST} percentile for SNPs with heterozygosities 0.45 to 0.5.

Microsatellite data were downloaded from N. Rosenberg's Web site, <http://www.cmb.usc.edu/people/noahr/diversity.html>, in *structure* format. The Rosenberg data lacked a population to match to our Ethiopian population, but data for 193 of the 377 loci were available from the dataset of Kayser et al. [65]. To represent our populations, we selected the populations in the Rosenberg data that are geographically coincident or proximate. As the distributions are quite similar for all populations (Figure 4B and 4C), the precision of population matching appears unimportant (also found by [65]). We selected as follows from the Rosenberg et al. data: Cameroon: Yoruba; China: Han Chinese; India: pooled samples from the populations included in Rosenberg et al.'s South Asia cluster, specifically Brahui, Balochi, Hazara, Makrani, Sindhi, Pathan, and Burusho; Italy: pooled samples from Sardinia, Tuscany, and Bergamo; Papua New Guinea: Papuan. For each microsatellite locus, expected heterozygosity was calculated as $(\frac{n}{n-1}) \sum_{i=1}^K (1-p_k^2)$, where n is the number of chromosomes sampled, K is the number of alleles, and p_k is the frequency of the k th allele. Repeat-number variance was calculated as

$$\left(\frac{1}{n-1}\right) \left(\sum_{i=1}^n x^2 - \frac{(\sum_{i=1}^n x)^2}{n} \right),$$

where x is the number of repeats in the n th chromosome.

The statistical properties of $\ln RV$ and $\ln RH$ allow us to estimate

significance values in a parametric context, reducing the influence of any non-neutral outliers in the tails of the empirical distribution. Each of the five $\ln RV$ distributions is consistent with normality, according to a Kolmogorov-Smirnov test. Standardizing our observed test statistics according to the empirical mean and standard deviation, and using the tail probabilities of the standard normal distribution, we recover p -values nearly identical to those drawn from the empirical distribution (Italy: 0.034; India: 0.035; China: 0.016; Ethiopia: 0.119; Papua New Guinea: 0.236). Of the $\ln RH$ distributions, only the Ethiopian sample conforms to normality according to the Kolmogorov-Smirnov test, conferring a parametric p -value of 0.0002 on the Ethiopian *PDYN* microsatellite.

The causes of the departures of $\ln RH$ from normality are unclear, but ascertainment bias is an obvious possibility. The 377 microsatellites were ascertained in a European population and may be biased against microsatellites with low heterozygosity in Europe. In general, ascertainment bias is expected to be very modest for microsatellites because low-heterozygosity microsatellites are quite rare [62,64,77]. As Rosenberg et al. [64] note, their microsatellite data are very similar to data from microsatellites ascertained in independent, geographically diverse panels. Nevertheless, we must consider the possibility that ascertainment bias contributes to the shapes of the empirical $\ln RV$ and $\ln RH$ distributions. The expected effect of ascertainment bias is the truncation of the left tails of the distributions, due to the exclusion of loci with low heterozygosity in Europeans, and consequently the extension of the right tails. Two predictions are thus a departure from normality and a significantly positive skew, measured by the third moment about the mean. As noted, all $\ln RV$ distributions are consistent with normality and have well-behaved tail probabilities. Only the Ethiopian $\ln RV$ distribution has a significantly positive skew. For $\ln RH$, four of five distributions fail the Kolmogorov-Smirnov test for normality, but the departures appear to be due largely to elevated kurtosis, not to positive skew. Only the Italian distribution has a significantly positive skew. We can construct a conservative test by drawing p -values from the right tails of the $\ln RH$ distributions, which should be enlarged relative to the unbiased case; all $\ln R\theta$ values are as extreme relative to the right tails as to the left, except for Ethiopian $\ln R\theta$ values, whose p -values rise to 0.016 ($\ln RH$) and 0.119 ($\ln RV$). Because $\ln RH$ has a smaller coalescent variance than $\ln RV$, $\ln RH$ is exquisitely sensitive to selection [63], and the observed departures from normality may therefore simply reflect the occurrence of selection at sites linked to some subset of the 377 loci [65,78]. The complete microsatellite dataset is presented in Table S2.

Supporting Information

Figure S1. Intensity of Positive Selection

The average selection coefficient (s) of advantageous mutations can be estimated from the rate acceleration of the human 68-bp element, conditioned on the fractions of all mutations that are advantageous, neutral, and deleterious. When the advantageous fraction is more than 2.5%, the average selection coefficient is less than 0.01. Over most of the parameter space, s is less than 0.001. The red line illustrates the case in which all and only the five fixed mutations are advantageous.

Found at DOI: 10.1371/journal.pbio.0030387.sg001 (1.7 MB EPS).

Table S1. Experimentally Determined *PDYN* Haplotypes from 74 Austrian Chromosomes

Each unique haplotype is shown, from a sample of chromosomes selected to overrepresent the rare one- and four-repeat alleles. Derived alleles are highlighted in red. Haplotypes were determined by complete sequencing of multiple clones of each allele. Msat refers to the CA_n microsatellite 1.3 kb upstream of the 68-bp repeat. Position 2370 segregates TC₇ and TC₉ alleles. The ancestral states at Msat and 2370 are uncertain, as both sites vary among and within the other primate species.

Found at DOI: 10.1371/journal.pbio.0030387.st001 (74 KB PDF).

Table S2. Microsatellite Summary Statistics

For the *PDYN* microsatellite and those used to generate the genome-wide empirical distributions, we report the sample sizes, expected heterozygosities, and repeat-number variances, as well as the test statistics $\ln RH$ and $\ln RV$.

Found at DOI: 10.1371/journal.pbio.0030387.st002 (223 KB XLS).

Accession Numbers

DNA sequences have been submitted to GenBank (<http://www.ncbi.nlm.nih.gov/Genbank>) with accession numbers AY902542–AY902679.

Acknowledgments

We thank Lisa Bukovnik, Manny Lopez, and Anjali Patel for assistance in the lab and Cliff Cunningham, Greg Gibson, Fred Nijhout, and Mark Rausher for helpful comments. Thanks to Mark

Stoneking for sharing data. This work was supported by a Royal Society/Wolfson Research Merit Award to DBG, and by grants and fellowships from the Leverhulme Trust to NS and DBG, the National Science Foundation to MVR, MWH, and GAW, and NASA to GAW.

Competing interests. The authors have declared that no competing interests exist.

Author contributions. MVR, MWH, NS, FZ, DBG, and GAW conceived and designed the experiments, performed the experiments, analyzed the data, contributed reagents/materials/analysis tools, and wrote the paper. ■

References

1. Chou HH, Hayakawa T, Diaz S, Krings M, Indriati E, et al. (2002) Inactivation of CMP-N-acetylneuraminic acid hydroxylase occurred prior to brain expansion during human evolution. *Proc Natl Acad Sci U S A* 99: 11736–11741.
2. Stedman HH, Kozyak BW, Nelson A, Thesier DM, Su LT, et al. (2004) Myosin gene mutation correlates with anatomical changes in the human lineage. *Nature* 428: 415–418.
3. Winter H, Langbein L, Krawczak M, Cooper DN, Jave-Suarez LF, et al. (2001) Human type I hair keratin pseudogene pihHaA has functional orthologs in the chimpanzee and gorilla: Evidence for recent inactivation of the human gene after the Pan-Homo divergence. *Hum Genet* 108: 37–42.
4. Fortna A, Kim Y, MacLaren E, Marshall K, Hahn G, et al. (2004) Lineage-specific gene duplication and loss in human and great ape evolution. *PLoS Biol* 2: e207. DOI: 10.1371/journal.pbio.0020207
5. Enard W, Przeworski M, Fisher SE, Lai CS, Wiebe V, et al. (2002) Molecular evolution of FOXP2, a gene involved in speech and language. *Nature* 418: 869–872.
6. Andres AM, Soldevila M, Navarro A, Kidd KK, Oliva B, et al. (2004) Positive selection in MAOA gene is human exclusive: Determination of the putative amino acid change selected in the human lineage. *Hum Genet* 5: 377–386.
7. Zhang J (2003) Evolution of the human ASPM gene, a major determinant of brain size. *Genetics* 165: 2063–2070.
8. Ferland RJ, Eyaid W, Collura RV, Tully LD, Hill RS, et al. (2004) Abnormal cerebellar development and axonal decussation due to mutations in AH11 in Joubert syndrome. *Nat Genet* 36: 1008–1013.
9. Evans PD, Anderson JR, Vallender EJ, Choi SS, Lahn BT (2004) Reconstructing the evolutionary history of microcephalin, a gene controlling human brain size. *Hum Mol Genet* 13: 1139–1145.
10. Huby T, Dacht C, Lawn RM, Wickings J, Chapman MJ, et al. (2001) Functional analysis of the chimpanzee and human apo(a) promoter sequences: Identification of sequence variations responsible for elevated transcriptional activity in chimpanzee. *J Biol Chem* 276: 22209–22214.
11. Heissig F, Krause J, Bryk J, Khaitovich P, Enard W, et al. (2005) Functional analysis of human and chimpanzee promoters. *Genome Biol* 6: R57.
12. Clark AG, Glanowski S, Nielsen R, Thomas PD, Kejariwal A, et al. (2003) Inferring nonneutral evolution from human-chimp-mouse orthologous gene trios. *Science* 302: 1960–1963.
13. Nielsen R, Bustamante C, Clark AG, Glanowski S, Sackton TB, et al. (2005) A scan for positively selected genes in the genomes of humans and chimpanzees. *PLoS Biol* 3: e170. DOI: 10.1371/journal.pbio.0030170
14. Dorus S, Vallender EJ, Evans PD, Anderson JR, Gilbert SL, et al. (2004) Accelerated evolution of nervous system genes in the origin of *Homo sapiens*. *Cell* 119: 1027–1040.
15. Hahn MW, Rockman MV, Soranzo N, Goldstein DB, Wray GA (2004) Population genetic and phylogenetic evidence for positive selection on regulatory mutations at the factor VII locus in humans. *Genetics* 167: 867–877.
16. Lowe CJ, Wray GA (1997) Radical alterations in the roles of homeobox genes during echinoderm evolution. *Nature* 389: 718–721.
17. Stern DL (2000) Evolutionary developmental biology and the problem of variation. *Evolution Int J Org Evolution* 54: 1079–1091.
18. Carroll SB, Grenier JK, Weatherbee SD (2001) From DNA to diversity: Molecular genetics and the evolution of animal design. London: Blackwell Science. 214 p.
19. Davidson EH (2001) Genomic regulatory systems: Development and evolution. San Diego: Academic Press. 261 p.
20. Wray GA, Hahn MW, Abouheif E, Balhoff JP, Pizer M, et al. (2003) The evolution of transcriptional regulation in eukaryotes. *Mol Biol Evol* 20: 1377–1419.
21. King MC, Wilson AC (1975) Evolution at two levels in humans and chimpanzees. *Science* 188: 107–116.
22. Carroll SB (2005) Evolution at two levels: On genes and form. *PLoS Biol* 3: e245. DOI: 10.1371/journal.pbio.0030245
23. Enard W, Khaitovich P, Klose J, Zollner S, Heissig F, et al. (2002) Intra- and interspecific variation in primate gene expression patterns. *Science* 296: 340–343.
24. Hsieh WP, Chu TM, Wolfinger RD, Gibson G (2003) Mixed-model reanalysis of primate data suggests tissue and species biases in oligonucleotide-based gene expression profiles. *Genetics* 165: 747–757.
25. Karaman MW, Houck ML, Chemnick LG, Nagpal S, Chawannakul D, et al. (2003) Comparative analysis of gene-expression patterns in human and African great ape cultured fibroblasts. *Genome Res* 13: 1619–1630.
26. Caceres M, Lachuer J, Zapala MA, Redmond JC, Kudo L, et al. (2003) Elevated gene expression levels distinguish human from non-human primate brains. *Proc Natl Acad Sci U S A* 100: 13030–13035.
27. Rockman MV, Wray GA (2002) Abundant raw material for cis-regulatory evolution in humans. *Mol Biol Evol* 19: 1991–2004.
28. Hoogendoorn B, Coleman SL, Guy CA, Smith K, Bowen T, et al. (2003) Functional analysis of human promoter polymorphisms. *Hum Mol Genet* 12: 2249–2254.
29. Buckland PR, Hoogendoorn B, Guy CA, Coleman SL, Smith SK, et al. (2004) A high proportion of polymorphisms in the promoters of brain expressed genes influences transcriptional activity. *Biochim Biophys Acta* 1690: 238–249.
30. Horan M, Millar DS, Hedderich J, Lewis G, Newsday V, et al. (2003) Human growth hormone 1 (GH1) gene expression: Complex haplotype-dependent influence of polymorphic variation in the proximal promoter and locus control region. *Hum Mutat* 21: 408–423.
31. Cheng HY, Pitcher GM, Laviolette SR, Whishaw IQ, Tong KI, et al. (2002) DREAM is a critical transcriptional repressor for pain modulation. *Cell* 108: 31–43.
32. Rodgers RJ, Cooper SJ, editors (1988) Endorphins, opiates and behavioural processes. New York: Wiley. 361 p.
33. Moles A, Kieffer BL, D'Amato FR (2004) Deficit in attachment behavior in mice lacking the mu-opioid receptor gene. *Science* 304: 1983–1986.
34. Wagner JJ, Terman GW, Chavkin C (1993) Endogenous dynorphins inhibit excitatory neurotransmission and block LTP induction in the hippocampus. *Nature* 363: 451–454.
35. Roth BL, Baner K, Westkaemper R, Siebert D, Rice KC, et al. (2002) Salvinorin A: A potent naturally occurring nonnitrogenous kappa opioid selective agonist. *Proc Natl Acad Sci U S A* 99: 11934–11939.
36. Zimprich A, Kraus J, Woltje M, Mayer P, Rauch E, et al. (2000) An allelic variation in the human prodynorphin gene promoter alters stimulus-induced expression. *J Neurochem* 74: 472–477.
37. Ventriglia M, Bocchio Chiavetto L, Bonvicini C, Tura GB, Bignotti S, et al. (2002) Allelic variation in the human prodynorphin gene promoter and schizophrenia. *Neuropsychobiology* 46: 17–21.
38. Chen AC, LaForge KS, Ho A, McHugh PF, Kellogg S, et al. (2002) Potentially functional polymorphism in the promoter region of prodynorphin gene may be associated with protection against cocaine dependence or abuse. *Am J Med Genet* 114: 429–435.
39. Stogmann E, Zimprich A, Baumgartner C, Aull-Watschinger S, Holtt V, et al. (2002) A functional polymorphism in the prodynorphin gene promoter is associated with temporal lobe epilepsy. *Ann Neurol* 51: 260–263.
40. Hurd YL (2002) Subjects with major depression or bipolar disorder show reduction of prodynorphin mRNA expression in discrete nuclei of the amygdaloid complex. *Mol Psychiatry* 7: 75–81.
41. Hurd YL, Herkenham M (1993) Molecular alterations in the neostriatum of human cocaine addicts. *Synapse* 13: 357–369.
42. Solbrig MV, Koob GF (2004) Epilepsy, CNS viral injury, and dynorphin. *Trends Pharmacol Sci* 25: 98–104.
43. Watanabe H, Fujiyama A, Hattori M, Taylor TD, Toyoda A, et al. (2004) DNA sequence and comparative analysis of chimpanzee chromosome 22. *Nature* 429: 382–388.
44. Yi S, Ellsworth DL, Li WH (2002) Slow molecular clocks in Old World monkeys, apes, and humans. *Mol Biol Evol* 19: 2191–2198.
45. Felsenstein J (1981) Evolutionary trees from DNA sequences: A maximum likelihood approach. *J Mol Evol* 17: 368–376.
46. Muse SV, Gaut BS (1997) Comparing patterns of nucleotide substitution rates among chloroplast loci using the relative ratio test. *Genetics* 146: 393–399.
47. Yang Z, Nielsen R, Goldman N, Pedersen AM (2000) Codon-substitution models for heterogeneous selection pressure at amino acid sites. *Genetics* 155: 431–449.
48. Maynard Smith J, Haigh J (1974) The hitch-hiking effect of a favourable gene. *Genet Res* 23: 23–35.
49. Fay JC, Wu CI (2000) Hitchhiking under positive Darwinian selection. *Genetics* 155: 1405–1413.
50. Kimura M (1983) The neutral theory of molecular evolution. Cambridge: Cambridge University Press. 367 p.

51. Haldane JBS (1927) The mathematical theory of natural and artificial selection. *Proc Camb Philos Soc* 23: 838–844.
52. Yu N, Jensen-Seaman MI, Chemnick L, Kidd JR, Deinard AS, et al. (2003) Low nucleotide diversity in chimpanzees and bonobos. *Genetics* 164: 1511–1518.
53. Bersaglieri T, Sabeti PC, Patterson N, Vanderploeg T, Schaffner SF, et al. (2004) Genetic signatures of strong recent positive selection at the lactase gene. *Am J Hum Genet* 74: 1111–1120.
54. Tishkoff SA, Varkonyi R, Cahinhinan N, Abbas S, Argyropoulos G, et al. (2001) Haplotype diversity and linkage disequilibrium at human G6PD: Recent origin of alleles that confer malarial resistance. *Science* 293: 455–462.
55. Carrion AM, Link WA, Ledo F, Mellstrom B, Naranjo JR (1999) DREAM is a Ca²⁺-regulated transcriptional repressor. *Nature* 398: 80–84.
56. Storz JF (2005) Using genome scans of DNA polymorphism to infer adaptive population divergence. *Mol Ecol* 14: 671–688.
57. Lewontin RC, Krakauer J (1973) Distribution of gene frequency as a test of the theory of the selective neutrality of polymorphisms. *Genetics* 74: 175–195.
58. Rockman MV, Hahn MW, Soranzo N, Goldstein DB, Wray GA (2003) Positive selection on a human-specific transcription factor binding site regulating IL4 expression. *Curr Biol* 13: 2118–2123.
59. Hinds DA, Stuve LL, Nilsen GB, Halperin E, Eskin E, et al. (2005) Whole-genome patterns of common DNA variation in three human populations. *Science* 307: 1072–1079.
60. Vallenius T, Makela TP (2002) Clik1: A novel kinase targeted to actin stress fibers by the CLP-36 PDZ-LIM protein. *J Cell Sci* 115: 2067–2073.
61. Ohta T, Kimura M (1973) A model of mutation appropriate to estimate the number of electrophoretically detectable alleles in a finite population. *Genet Res* 22: 201–204.
62. Schlotterer C (2002) A microsatellite-based multilocus screen for the identification of local selective sweeps. *Genetics* 160: 753–763.
63. Kauer MO, Dieringer D, Schlotterer C (2003) A microsatellite variability screen for positive selection associated with the “out of Africa” habitat expansion of *Drosophila melanogaster*. *Genetics* 165: 1137–1148.
64. Rosenberg NA, Pritchard JK, Weber JL, Cann HM, Kidd KK, et al. (2002) Genetic structure of human populations. *Science* 298: 2381–2385.
65. Kayser M, Brauer S, Stoneking M (2003) A genome scan to detect candidate regions influenced by local natural selection in human populations. *Mol Biol Evol* 20: 893–900.
66. Han JS (2004) Acupuncture and endorphins. *Neurosci Lett* 361: 258–261.
67. Saetre P, Lindberg J, Leonard JA, Olsson K, Pettersson U, et al. (2004) From wild wolf to domestic dog: Gene expression changes in the brain. *Brain Res Mol Brain Res* 126: 198–206.
68. Lim MM, Wang Z, Olazabal DE, Ren X, Terwilliger EF, et al. (2004) Enhanced partner preference in a promiscuous species by manipulating the expression of a single gene. *Nature* 429: 754–757.
69. Oliver F, Christians JK, Liu X, Rhind S, Verma V, et al. (2005) Regulatory variation at glypican-3 underlies a major growth QTL in mice. *PLoS Biol* 3: e135. DOI: 10.1371/journal.pbio.0030135
70. Posada D, Crandall KA (1998) MODELTEST: Testing the model of DNA substitution. *Bioinformatics* 14: 817–818.
71. Hudson RR, Kaplan NL (1986) On the divergence of alleles in nested subsamples from finite populations. *Genetics* 113: 1057–1076.
72. Rozas J, Rozas R (1999) DnaSP version 3: An integrated program for molecular population genetics and molecular evolution analysis. *Bioinformatics* 15: 174–175.
73. Nei M (1987) *Molecular evolutionary genetics*. New York: Columbia University Press. 512 p.
74. Otto SP, Whitlock MC (1997) The probability of fixation in populations of changing size. *Genetics* 146: 723–733.
75. Nagylaki T, Petes TD (1982) Intrachromosomal gene conversion and the maintenance of sequence homogeneity among repeated genes. *Genetics* 100: 315–337.
76. Walsh JB (1986) Selection and biased gene conversion in a multigene family: Consequences of interallelic bias and threshold selection. *Genetics* 112: 699–716.
77. Weissenbach J, Gyapay G, Dib C, Vignal A, Morissette J, et al. (1992) A second-generation linkage map of the human genome. *Nature* 359: 794–801.
78. Storz JF, Payseur BA, Nachman MW (2004) Genome scans of DNA variability in humans reveal evidence for selective sweeps outside of Africa. *Mol Biol Evol* 21: 1800–1811.
79. Kent WJ, Sugnet CW, Furey TS, Roskin KM, Pringle TH, et al. (2002) The human genome browser at UCSC. *Genome Res* 12: 996–1006.